TRANSPORT ACROSS HOMOPOROUS AND HETEROPOROUS MEMBRANES IN NONIDEAL, NONDILUTE SOLUTIONS

II. Inequality of Phenomenological and Tracer Solute Permeabilities

M. H. Friedman and R. A. Meyer, *Applied Physics Laboratory, The Johns Hopkins University, Laurel, Maryland 20810*

ABSTRACT The phenomenological solute permeability (ω_P) of a membrane measures the flux of solute across it when the concentrations of the solutions on the two sides of the membrane differ. The relationship between ω_P and the conventionally measured tracer permeability (ω_T) is examined for homoporous and heteroporous (parallel path) membranes in nonideal, nondilute solutions and in the presence of boundary layers. In general, ω_P and ω_T are not equal; therefore, predictions of transmembrane solute flux based on ω_T are always subject to error. For a homoporous membrane, the two permeabilities become equal as the solutions become ideal and dilute. For heteroporous membranes, ω_P is always greater than ω_T. An upper bound on $\omega_P - \omega_T$ is derived to provide an estimate of the maximum error in predicted solute flux. This bound is also used to show that the difference between ω_P and ω_T demonstrated earlier for the sucrose-Cuprophan system can be explained if the membrane is heteroporous. The expressions for ω_P developed here support the use of a modified osmotic driving force to describe membrane transport in nonideal, nondilute solutions.

INTRODUCTION

Two permeabilities have been used to characterize the flux of solute across membranes. The tracer solute permeability, ω_T, is conventionally determined from a measurement of the flux of a trace amount of radioactive solute in the absence of both a hydrostatic pressure difference and a concentration difference of the abundant nonradioactive solute. The phenomenological solute permeability, ω_P, describes the solute flux under a concentration gradient of the abundant species. Previous investigators (1–4) have shown that, if the bounding solutions are ideal and dilute and the membrane is homoporous, $\omega_T = \omega_P$; on the other hand, if the membrane consists of an array of parallel paths, $\omega_T \leq \omega_P$. The difference between ω_P and ω_T, which can be attributed to the circulation of flows across the parallel elements of the heteroporous array (5), implies that significant errors can result if tracer permeabilities are used to predict the solute flux driven by a concentration gradient across such a membrane (3). A difference between ω_P and ω_T has recently been demonstrated experimentally (6) for the solute-membrane system sucrose-Cuprophan 150PM. However, these experiments were carried out at sucrose concentrations up to 900 mM; therefore, before attributing this

difference to membrane heteroporosity, it is necessary to examine the influence of solution nonideality and nondiluteness on the relationship between the two permeabilities.

In the preceding paper (7), solute and volume flux equations were developed to demonstrate the effects of solution nonideality and nondiluteness on the relationship between the reflection coefficients for volume flow and solute flow. Here, these equations are used to examine the relationship between ω_P and ω_T. We find that, in nonideal, nondilute solutions, $\omega_P \neq \omega_T$, even for a homoporous membrane. The relationship between the permeabilities involves not only the properties of the solution, but the remaining membrane transport parameters as well. The presence of boundary layers does not affect this relationship for a homoporous membrane but generally reduces the difference between the permeabilities for a heteroporous membrane.

Since most membrane transport studies are performed with membranes of uncertain structure in solutions that are necessarily neither perfectly ideal nor infinitely dilute, the use of the conventionally measured tracer permeability to predict solute flux under a concentration gradient will always result in some error. An equation is provided to estimate, from conventionally measured transport properties, the maximum value of ω_P, and hence the maximum error in predicted solute flux. Using this equation, it is shown that the differences between ω_P and ω_T reported by Meyer et al. (6) for Cuprophan can be explained if the membrane is heteroporous.

NOTATION

The definitions, equations and symbols from reference 7 used below are summarized in this section. Equation numbers from reference 7 are prefixed by "I".

Definitions of Phenomenological Coefficients

The conventional phenomenological coefficients used here are defined by the following equations for the transport of a single nonelectrolyte:

$$J_v = -L_p(\Delta P - \sigma_v RT\Delta c_s) \tag{I1 a}$$

$$J_s = J_v(1 - \sigma_s)\bar{c}_s - \omega_P RT\Delta c_s. \tag{I1 b}$$

The signs of ΔP and Δc_s are opposite to those of the usual presentation, for consistency with the differential form (7). From these equations, the phenomenological coefficients are defined as follows:

$$\sigma_v \equiv \left.\frac{\Delta P}{RT\Delta c_s}\right|_{J_v=0}, \qquad \text{reflection coefficient for volume flow} \qquad \text{(Def. 1)}$$

$$\omega_P \equiv -\left.\frac{J_s}{RT\Delta c_s}\right|_{J_v=0}, \qquad \begin{array}{l}\text{phenomenological solute permeability}\\ \text{(also called solute permeability at}\\ \text{zero volume flow [8], and effective}\\ \text{solute permeability [3, 9])}\end{array} \qquad \text{(Def. 2)}$$

$$\sigma_s \equiv 1 - \left.\frac{J_s}{\bar{c}_s J_v}\right|_{\Delta c_s=0}, \qquad \text{reflection coefficient for solute flow} \qquad \text{(Def. 3)}$$

$$L_p \equiv -\left.\frac{J_v}{\Delta P}\right|_{\Delta c_s=0}, \qquad \text{hydraulic conductivity} \qquad \text{(Def. 4)}$$

$$\omega_T \equiv -\frac{J_s^*}{RT\Delta c_s^*}\bigg|_{\substack{J_v=0\\ \Delta c_s=0}}, \qquad \text{tracer solute permeability (asterisk indicates tracer species)} \qquad \text{(Def. 5)}$$

Flux Equations

The following solute and volume flux equations for nonideal, nondilute solutions were derived in reference 7.

$$J_s = \frac{1}{\mathcal{D}}\left[(\overline{V}_s r_{ww} - \overline{V}_w r_{sw})\Delta P + \frac{r_{ww}(1-\bar{\nu}_s) + \overline{V}_w \bar{c}_s r_{sw}}{\bar{c}_s(1-\bar{\nu}_s)}(1+\Gamma)RT\Delta c_s\right] \qquad \text{(I5 } a\text{)}$$

$$J_v = \frac{1}{\mathcal{D}}\left[(\overline{V}_w^2 r_{ss} - 2\overline{V}_w\overline{V}_s r_{sw} + \overline{V}_s^2 r_{ww})\Delta P - \frac{\overline{V}_w^2\bar{c}_s r_{ss} + \overline{V}_w r_{sw}(1-2\bar{\nu}_s) - \overline{V}_s r_{ww}(1-\bar{\nu}_s)}{\bar{c}_s(1-\bar{\nu}_s)}(1+\Gamma)RT\Delta c_s\right], \qquad \text{(I5 } b\text{)}$$

where $\mathcal{D} = r_{ss}r_{ww} - r_{sw}^2$.

Relationship between σ_v and σ_s

$$\sigma_s = \sigma_v\left(\frac{1-\bar{\nu}_s}{1+\Gamma}\right) \qquad \text{(I8)}$$

where

$$\sigma_v = \left(\frac{1+\Gamma}{1-\bar{\nu}_s}\right)\left[\frac{\overline{V}_w^2\bar{c}_s r_{ss} + \overline{V}_w r_{sw}(1-2\bar{\nu}_s) - \overline{V}_s r_{ww}(1-\bar{\nu}_s)}{\bar{c}_s(\overline{V}_w^2 r_{ss} - 2\overline{V}_w\overline{V}_s r_{sw} + \overline{V}_s^2 r_{ww})}\right]. \qquad \text{(I7 } b\text{)}$$

Symbols

a_i	activity of the ith species
c	total molar concentration
$c_s(x)$	solute concentration (abundant species)
$\bar{c}_s$	mean solute concentration
D_{ij}	multicomponent diffusivity of the species pair (i, j)
J_i	flux of the ith species, positive from left to right
J_v	volume flux, positive from left to right
$P(x)$	hydrostatic pressure
R	gas constant
$r_{ij} = RT\int_0^\alpha (cD_{ij})^{-1}dx$,	interaction coefficient between species i and j.
T	absolute temperature
$\overline{V}_i$	partial molar volume of the ith species
W_P	half of the phenomenological permeability of a single boundary layer
x	coordinate normal to membrane ($x = 0$ at left side, $x = \alpha$ at right side)
α	membrane thickness
$\Gamma = (\mathrm{d}\ln\gamma_s/\mathrm{d}\ln c_s)_{c_s=\bar{c}_s}$,	a measure of the influence of nonideality on the transport process
γ_s	activity coefficient of the solute
$\bar{\nu}_s = \overline{V}_s\bar{c}_s$,	a measure of the nondiluteness of the solutions bounding the membrane

Subscripts

s	solute
w	solvent (water)

Prefix

Δ	value at right side of membrane minus value at left side

Superscript and Subscript Notation Specific to Membrane Transport Properties (Illustrated by ω_P)

ω_P	value that would be measured in a boundary-layer-free experiment
ω'_P	value that would be measured in the presence of boundary layers; actual experimental value
$\omega_P^{(n)}$, $\omega_P'^{(n)}$	value that would be exhibited by an n-path membrane (specified in the text) in the absence and presence of boundary layers, respectively (this notation is used only for ω_P)
ω_{Pi}	property of the ith path in a heteroporous membrane

HOMOPOROUS MEMBRANE

In this section, the solute and volume flux equations (Eq. I5 *a* and *b*) are used to determine the relationship between ω_P and ω_T for a homoporous membrane in nonideal, nondilute solutions. Using the definitions in the preceding section, σ_v, L_p and ω_T are expressed in terms of the three interaction coefficients r_{ss}, r_{sw}, and r_{ww}. These expressions are inverted to obtain equations for each of the interaction coefficients in terms of these three phenomenological coefficients. Since ω_P can be written in terms of the interaction coefficients, it can also be written in terms of σ_v, L_p, and ω_T. It is found that $\omega_P \neq \omega_T$ and that ω_P is a function of σ_v, L_p, ω_T, Γ, and $\bar{\nu}_s$.

Phenomenological Coefficients in Terms of Interaction Coefficients

The expression for σ_v in terms of the interaction coefficients is given by Eq. I7 *b*. From Def. 4 and Eq. I5 *b*,

$$L_p = -(\bar{V}_w^2 r_{ss} - 2\bar{V}_w \bar{V}_s r_{sw} + \bar{V}_s^2 r_{ww})/(r_{ss} r_{ww} - r_{sw}^2). \tag{1}$$

The simplest experiment from which to develop the relationship between ω_T and the interaction coefficients is one in which $\Delta P = 0$ and the concentration of the abundant species on the "cold" side of the membrane ($x = 0$) equals the sum of the concentrations of the abundant and tracer species on the "hot" side ($x = \alpha$). Under these conditions, $dP/dx = 0$, $J_w = 0$, and $J_s + J_s^* = 0$, so $J_v = 0$. The total solute concentration, and hence the solute activity coefficient, are uniform, so $d \ln a_s = d \ln c_s$, and the Kirkwood formulation (7, 10) gives

$$\frac{1}{c_s}\frac{dc_s}{dx} = \frac{J_s}{cD_{ss}} + \frac{J_s^*}{cD_{ss^*}} \tag{2}$$

for the abundant species. The left-hand side of Eq. 2 integrates to $[c_s(\alpha) - c_s(0)]/\bar{c}_s$, where $\bar{c}_s \approx c_s(\alpha) \approx c_s(0)$; the integral of the right-hand side is $J_s r_{ss}/(RT)$ if isotope interaction effects are neglected ($r_{ss^*} = 0$). Since $c_s(\alpha) - c_s(0) = c_s^*(0) - c_s^*(\alpha) = -\Delta c_s^*$ and $J_s = -J_s^*$, the integrated form of Eq. 2 can be written as

$$\frac{\Delta c_s^*}{\bar{c}_s} = \frac{J_s^* r_{ss}}{RT}.$$

From Def. 5,

$$\omega_T = -\frac{1}{\bar{c}_s r_{ss}}. \tag{3}$$

Thus ω_T is inversely proportional to r_{ss} and independent of r_{sw} and r_{ww}.[1]

Interaction Coefficients in Terms of Phenomenological Coefficients

The equations for σ_v, L_p, and ω_T in terms of the interaction coefficients are now inverted to obtain equations for the interaction coefficients in terms of these phenomenological coefficients. From Eq. 3, r_{ss} is a simple function of ω_T:

$$r_{ss} = -\frac{1}{\bar{c}_s \omega_T}. \tag{4}$$

The equations for r_{sw} and r_{ww} are not as simple. Eq. I7 *b* is solved for r_{ww}, which is substituted into Eq. 1. Using Eq. 4, a quadratic expression for r_{sw} in terms of ω_T, σ_v, and L_p is obtained whose discriminant is a perfect square; the two roots are

$$r_{sw} = \frac{\bar{V}_w[-2L_p(1-\bar{\nu}_s)(1+\Gamma+\sigma_v\bar{\nu}_s) + (1+\Gamma)(L_p - \bar{V}_s\bar{\nu}_s\omega_T) \pm (1+\Gamma)(L_p - \bar{V}_s\bar{\nu}_s\omega_T)]}{2L_p\omega_T\bar{\nu}_s(1-\bar{\nu}_s)(1+\Gamma+\sigma_v\bar{\nu}_s)}.$$

The negative root, which gives $r_{sw} = -\bar{V}_w/(\omega_T\bar{\nu}_s) = \bar{V}_w r_{ss}/\bar{V}_s$, is rejected because r_{sw} and r_{ss} are independent; the positive root gives

$$r_{sw} = \frac{\bar{V}_w[(L_p - \bar{V}_s\omega_T)(1+\Gamma) - L_p\sigma_v(1-\bar{\nu}_s)]}{L_p\omega_T(1-\bar{\nu}_s)(1+\Gamma+\sigma_v\bar{\nu}_s)}. \tag{5}$$

Eq. 5 is substituted into the expression for r_{ww} obtained from Eq. I7 *b*, giving

$$r_{ww} = -\frac{\bar{V}_w^2\{(1+\Gamma)\omega_T[(1+\Gamma)(1-2\bar{\nu}_s) + 2\sigma_v\bar{\nu}_s(1-\bar{\nu}_s)] + L_p\bar{c}_s[1+\Gamma-\sigma_v(1-\bar{\nu}_s)]^2\}}{L_p\omega_T(1-\bar{\nu}_s)^2(1+\Gamma+\sigma_v\bar{\nu}_s)^2}. \tag{6}$$

Phenomenological Permeability in Terms of ω_T, L_p, and σ_v

The phenomenological permeability is defined (Def. 2) in terms of the solute flux when $J_v = 0$. Under this condition, Eq. I5 *a* becomes

$$J_s|_{J_v=0} = \frac{1}{\mathcal{D}}\left\{(\bar{V}_s r_{ww} - \bar{V}_w r_{sw})\sigma_v + \left[\frac{r_{ww}(1-\bar{\nu}_s) + \bar{V}_w\bar{c}_s r_{sw}}{\bar{c}_s}\right]\left[\frac{1+\Gamma}{1-\bar{\nu}_s}\right]\right\} RT\Delta c_s, \tag{7}$$

where Def. 1 has been used to replace ΔP by $\sigma_v RT\Delta c_s$. Eqs. 4–6 are substituted into Eq. 7;

[1]The relationship between ω_T and the interaction coefficients depends on the experimental technique used to measure the tracer permeability. Eq. 3 would not be expected to hold in the presence of substantial flows, such as that of solvent, to which the isotope flux could be coupled.

from the definition of ω_P,

$$\omega_P = \frac{(1 - \bar{\nu}_s)(1 + \Gamma + \sigma_v\bar{\nu}_s)^2}{(1 + \Gamma)\left(1 - \dfrac{\omega_T\bar{\nu}_s^2}{L_p\bar{c}_s}\right)}\omega_T. \tag{8 a}$$

Using the relationship between σ_s and σ_v (Eq. I8), this can also be written as

$$\omega_P = \left(\frac{1 + \Gamma}{1 - \bar{\nu}_s}\right)\frac{[1 - \bar{\nu}_s(1 - \sigma_s)]^2}{\left[1 - \dfrac{\omega_T\bar{\nu}_s^2}{L_p\bar{c}_s}\right]}\omega_T. \tag{8 b}$$

Note that $\omega_P \rightarrow \omega_T$ when Γ and $\bar{\nu}_s \rightarrow 0$. It is shown in Appendix A that $\omega_T\bar{\nu}_s^2/(L_p\bar{c}_s) \leq \bar{\nu}_s$, so the expression for ω_P is well behaved.

Eq. 8 *a* and *b* demonstrates the effects of nonideality and nondiluteness on the relationship between the phenomenological and tracer permeabilities which a homoporous membrane would exhibit if no boundary layers were present. The values of reflection coefficient and hydraulic conductivity which enter into Eq. 8 *a* and *b* are likewise those of the membrane alone. The relationship between the experimental permeabilities, measured with boundary layers present, is derived in Appendix B, with the interesting result that Eq. 8 *a* and *b* still hold, provided that experimental transport coefficients are used throughout.

HETEROPOROUS MEMBRANE

Previous analyses (1–4) have shown that ω_P can differ from ω_T for heteroporous (parallel path) membranes in ideal, dilute solutions. In this section, the equations derived in reference 7 for membrane transport in nonideal, nondilute solutions are used to examine the relationship between ω_P and ω_T for a heteroporous membrane.

Consider a heteroporous membrane consisting of n simple paths in parallel. The equations for volume and solute flux across the composite membrane in terms of the phenomenological coefficients of the individual paths are similar to those developed previously, except that the distinction between σ_v and σ_s is retained:

$$J_v = \sum_{i=1}^{n} J_{vi} = -\Delta P\Sigma L_{pi} + RT\Delta c_s\Sigma L_{pi}\sigma_{vi} \tag{9}$$

and

$$J_s = \sum_{i=1}^{n} J_{si} = \bar{c}_s\Sigma J_{vi}(1 - \sigma_{si}) - RT\Delta c_s\Sigma\omega_{Pi}$$

$$= -\bar{c}_s\Delta P\Sigma L_{pi}(1 - \sigma_{si}) + RT\Delta c_s[\bar{c}_s\Sigma L_{pi}\sigma_{vi}(1 - \sigma_{si}) - \Sigma\omega_{Pi}], \tag{10}$$

where the subscript i designates the ith path. From these equations, several "conservation" equations can be derived (1, 2) that relate the transport properties of the composite to those of the individual pathways through it:

$$L_p = \Sigma L_{pi} \tag{11 a}$$

$$L_p\sigma_v = \Sigma L_{pi}\sigma_{vi} \tag{11 b}$$

$$\omega_T = \Sigma\omega_{Ti}. \tag{11 c}$$

As shown in the preceding paper (7), the relationship between σ_v and σ_s (Eq. I8) holds for both simple and heteroporous membranes; thus, Eq. (11 *b*) can also be written as

$$L_p\sigma_s = \Sigma L_{pi}\sigma_{si}. \tag{11 d}$$

The relationship between the phenomenological permeabilities of each path and that of the composite is less simple than Eq. 11 *c*. Eq. 9 is solved for ΔP when $J_v = 0$, this is substituted into Eq. 10, and Def. 2 is used to obtain

$$\omega_P = -\frac{\bar{c}_s\Sigma L_{pi}\sigma_{vi}\Sigma L_{pi}\sigma_{si}}{\Sigma L_{pi}} + \bar{c}_s\Sigma L_{pi}\sigma_{vi}\sigma_{si} + \Sigma\omega_{Pi}. \tag{12}$$

Using Eq. 11 *a*, *b* and *d*, Eq. 12 simplifies to

$$\omega_P = -\bar{c}_s L_p\sigma_v\sigma_s + \bar{c}_s\Sigma L_{pi}\sigma_{vi}\sigma_{si} + \Sigma\omega_{Pi}. \tag{13}$$

Since σ_v and σ_s are simply related, Eq. 13 can be written in terms of either variable. The modified Kedem-Katchalsky equations, derived in the preceding paper (reference 7, Eq. 9 *a* and *b*), suggest that σ_s is the more "natural" variable. Accordingly, we write Eq. 13 in terms of this coefficient:

$$\omega_P = \left(\frac{1+\Gamma}{1-\bar{\nu}_s}\right)\left[-\bar{c}_s L_p\sigma_s^2 + \bar{c}_s\Sigma L_{pi}\sigma_{si}^2\right] + \Sigma\omega_{Pi}, \tag{14}$$

where, from Eq. 8 *b*,

$$\Sigma\omega_{Pi} = \left(\frac{1+\Gamma}{1-\bar{\nu}_s}\right)\Sigma\frac{[1-\bar{\nu}_s(1-\sigma_{si})]^2}{1-\dfrac{\omega_{Ti}\bar{\nu}_s^2}{L_{pi}\bar{c}_s}}\omega_{Ti}.$$

The effects of heteroporosity and nonideality on ω_P can easily be identified in Eq. 14. The effect of heteroporosity is represented by the bracketed term, which is positive and can be related to the variance of the appropriately weighted reflection coefficients of the constituent pathways, exactly as for the ideal case (3). This "heteroreflectivity" term is multiplied by a factor $(1+\Gamma)/(1-\bar{\nu}_s)$, which measures the nonideality and nondiluteness of the solutions bounding the membrane. For ideal dilute solutions, $\omega_{Pi} = \omega_{Ti}$ and (from Eq. 11 *c*) $\Sigma\omega_{Pi} = \omega_T$; however, as can be seen above, the summation is more complex in concentrated solutions.

Since ω_P is generally not equal to ω_T, predictions of solute flux under a concentration gradient that use ω_T instead of ω_P in Eq. I1 *b* are subject to error. Since the effect of heteroporosity is to increase ω_P, the possible importance of this error can be assessed by examining the maximum ω_P of a multipath membrane whose experimental coefficients ω_T', L_p', and σ_s' (or σ_v') are given.

Two-Path Membrane

It has been shown (3) that the heteroreflectivity term in Eq. 14 has its largest value when some of the pores are impermeable to the solute ($\sigma_{si} = 1$) and the remainder of the pores are

nonselective toward the solute ($\sigma_{si} = 0$). Thus, as a first estimate of the maximum ω_P, we consider a two-path membrane whose properties are tabulated below:

Path 1	Path 2
$\sigma_{s1} = 1$	$\sigma_{s2} = 0$
$\omega_{T1} = 0$	$\omega_{T2} = \omega'_T$
$L_{p1} = L'_p\sigma'_s$	$L_{p2} = L'_p(1 - \sigma'_s)$

Here, boundary layers are assumed to be absent, so the (primed) experimental phenomenological coefficients of the composite membrane can be equated to the unprimed coefficients (see Notation), and the conservation equations (Eq. 11 *a–d*) are satisfied. From Eq. 14, the phenomenological permeability of the two-path composite membrane is

$$\omega_P^{(2)} = \left(\frac{1 + \Gamma}{1 - \bar{\nu}_s}\right)\left\{L'_p\bar{c}_s\sigma'_s(1 - \sigma'_s) + \frac{\omega'_T(1 - \bar{\nu}_s)^2}{\left[1 - \frac{\omega'_T\bar{\nu}_s^2}{L'_p(1 - \sigma'_s)\bar{c}_s}\right]}\right\}. \tag{15}$$

Three-Path Membrane

The difference between ω_P and ω_T can be increased beyond that given by Eq. 15 if path 2 above is replaced by two nonselective paths whose hydraulic conductivities and tracer permeabilities are selected to maximize $\Sigma\omega_{Pi}$ in Eq. 14. The details of this analysis are given in Appendix C. The resulting equation for the phenomenological permeability of the three-path membrane, in the absence of boundary layers, is

$$\omega_P^{(3)} = \left(\frac{1 + \Gamma}{1 - \bar{\nu}_s}\right)L'_p\bar{c}_s\sigma'_s(1 - \sigma'_s) + \omega'_T(1 + \Gamma) = L'_p\bar{c}_s\sigma'_v(1 - \sigma'_s) + \omega'_T(1 + \Gamma). \tag{16}$$

Equations 15 and 16 can be used to estimate the error in solute flux prediction that might result if the membrane is heteroporous and the tracer permeability is used in Eq. 11 *b* instead of the phenomenological permeability. It appears that Eq. 16 provides an upper bound on this error. The effect of boundary layer thickness on the phenomenological permeability of the model three-path membrane is analyzed in the latter part of Appendix C. This analysis shows that, unlike the homoporous membrane case (Appendix B), the difference between the experimentally measured phenomenological and tracer permeabilities of this heteroporous membrane is generally reduced by the presence of unstirred boundary layers.

DISCUSSION

The phenomenological solute permeability, ω_P, which describes the flux of solute under its concentration gradient, is in general not equal to the conventionally measured tracer solute permeability, ω_T. For simple homoporous membranes, the difference between ω_P and ω_T given by Eq. 8 *a* and *b* is related to the ideality and diluteness of the bounding solutions; ω_P approaches ω_T as the solutions become more ideal ($\Gamma \rightarrow 0$) and more dilute ($\bar{\nu}_s \rightarrow 0$). For heteroporous membranes, an additional "heteroreflectivity" term appears in the expression for ω_P (Eq. 14). This term, described previously for ideal, dilute solutions (2, 3), is related to the reflection coefficients of the individual pathways and is maximized when some paths are impermeable to solute ($\sigma_{si} = 1$) and the remaining paths are nonselective to solute ($\sigma_{si} = 0$)

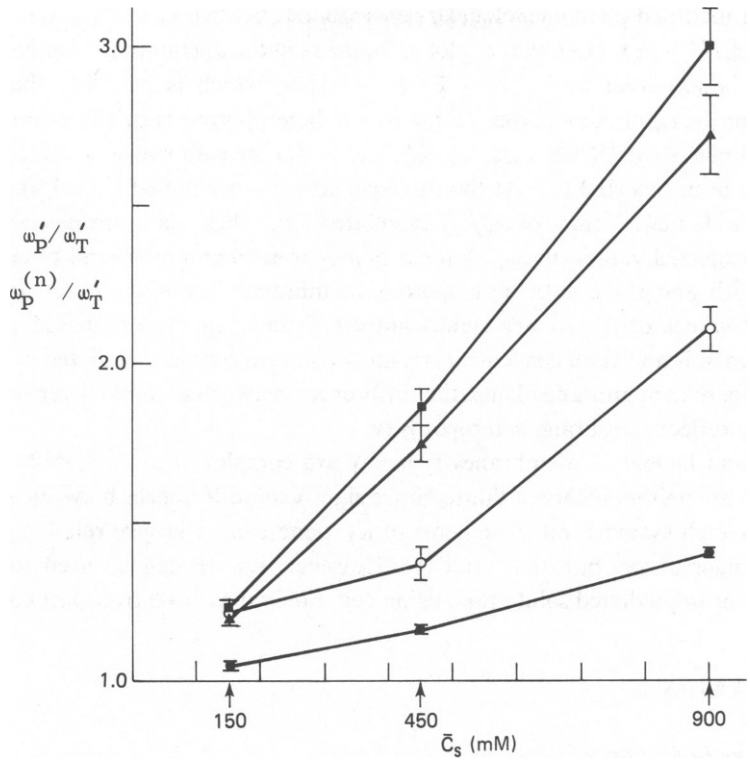

FIGURE 1 Ratio of experimental or predicted phenomenological solute permeability (ω_P' or $\omega_P^{(n)}$) to experimental tracer solute permeability (ω_T') vs. mean solute concentration ($\bar{c}_s$), for the sucrose-Cuprophan system. (○) Experimental data (6); (●) homoporous membrane; (▲) model two-path heteroporous membrane; (■) model three-path heteroporous membrane. For the homoporous and model heteroporous membranes, the phenomenological permeability is given by Eqs. B10, 15, or 16, using the measured (6) ω_T', L_p', and σ_v'. Eq. I8, verified experimentally in reference 7 for the sucrose-Cuprophan system, was used to calculate σ_s' from σ_v'; the needed values of Γ and $\bar{\nu}_s$ were taken from reference 7.

(3). The heteroreflectivity term is multiplied by a concentration-dependent factor that approaches unity as the bounding solutions become more ideal and dilute.

In physical terms, that portion of the difference between ω_P and ω_T not due to solution nonideality arises because the volume flows through the paths in a heteroporous membrane are generally different for each permeability measurement. This is so even though $J_v = 0$ in both cases. When ω_T is measured, the volume flow in each path is zero; however, in an ω_P experiment, there may be nonzero flows through individual paths, though their sum is zero. The "circulation" of volume flow among the different paths in the latter case can result in a contribution to the solute flow when the reflection coefficients of the individual paths are different; this leads to an increase in the effective membrane permeability (1).

In the preceding paper (7), we showed that by defining a modified osmotic driving force the equations for volume and solute flux in nonideal, nondilute solutions can be written in a form similar to the equations for transport in ideal solutions. The flux equations are

$$J_v = -L_p(\Delta P - \sigma_s \Delta \pi_s) \qquad (17\,a)$$

$$J_s = J_v(1 - \sigma_s)\bar{c}_s - \tilde{\omega}_P \Delta \pi_s, \qquad (17\,b)$$

where $\tilde{\omega}_P$ is a modified phenomenological permeability, defined as $(-J_s/\Delta\pi_s)_{J_v=0}$, and $\Delta\pi_s = (1 + \Gamma)RT\Delta c_s/(1 - \bar{\nu}_s)$. Note that σ_s, not σ_v, appears in the J_v equation. Comparing Eqs. I1 *b* and 17 *b*, it is seen that $\omega_P = [(1 + \Gamma)/(1 - \bar{\nu}_s)]\tilde{\omega}_P$, which is precisely the form of the expressions for the ω_P of homoporous (Eq. 8 *b*) and heteroporous (Eq. 14) membranes.

The experimental coefficients ω'_P, ω'_T, L'_p, and σ'_v for sucrose transport across Cuprophan have recently been reported (6). At the three concentrations studied ($\bar{c}_s$ = 150, 450, and 900 mM), ω'_P exceeded ω'_T. Values of ω'_P/ω'_T calculated from these data are plotted against $\bar{c}_s$ in Fig. 1. The expected values of ω'_P/ω'_T for a homoporous membrane, and of $\omega_P^{(n)}/\omega'_T$ for the model two-path and three-path heteroporous membranes, are also plotted in Fig. 1. The experimental values of ω'_P/ω'_T are significantly greater than the calculated values for the homoporous membrane at all concentrations and do not exceed the calculated values for either model heteroporous membrane. Thus, the differences between ω'_P and ω'_T reported by Meyer et al. (6) may reflect membrane heteroporosity.

Artificial and biological membranes typically are complex structures that are studied in solutions that are neither ideal nor dilute. Since significant differences between ω_P and ω_T may be present in such systems, measurements of ω_T alone cannot ensure reliable predictions of solute flux under a concentration gradient. However, Eq. 16 can be used to estimate the maximum error in predicted solute flux, using commonly measured transport coefficients.

APPENDIX A

Upper Bound on $\omega_T\bar{\nu}_s^2/(L_p\bar{c}_s)$

The expressions derived in the body of this paper allow $\omega_T\bar{\nu}_s^2/(L_p\bar{c}_s)$ to be expressed in terms of any combination of phenomenological and interaction coefficients. The bound on this ratio must follow from *a priori* bounds on the coefficients chosen. A convenient first assumption of this kind is that the reflection coefficients of the membrane are non-negative. Thus, Eqs. 1 and 3 are used to express the ratio in terms of interaction coefficients, and Eqs. I7 *b* and I8 are used to replace r_{ww} with σ_s. The result is

$$\frac{\omega_T\bar{\nu}_s^2}{L_p\bar{c}_s} = \bar{\nu}_s(1 - \sigma_s) + \frac{\bar{V}_s r_{sw}}{\bar{V}_w r_{ss}}[1 - \bar{\nu}_s(1 - \sigma_s)].$$

The ratio is regarded as a function of three independent coefficients: σ_s, r_{ss}, and r_{sw}. Since $\infty > \omega_T \geq 0$, it follows from Eq. 4 that $r_{ss} < 0$. It is then reasonable to expect that the cross-coefficient r_{sw} is of opposite sign (11), and indeed, numerical evaluations of r_{sw}, using the experimental data of Meyer et al. (6), confirm that $r_{sw} > 0$. With these inequalities, it is seen that the ratio of interest is maximized when $\sigma_s = 0$ and $r_{sw} \to 0$:

$$\left(\frac{\omega_T\bar{\nu}_s^2}{L_p\bar{c}_s}\right)_{max} = \bar{\nu}_s.$$

APPENDIX B

Phenomenological Coefficients of a Homoporous Membrane with Boundary Layers

Consider a homoporous membrane bounded by boundary layers of a finite thickness. Assume that the reflection coefficients of, and pressure drops across, the boundary layers are zero. The analysis of

transport across this system proceeds similarly to that described in Appendix A of reference 7 but with the simplification that only a single path need be considered. Eq. 8 *a* does, however, predict a difference between the tracer and phenomenological permeabilities of the boundary layer; when $\sigma_v = 0$ and L_p becomes large,

$$W_P = (1 - \bar{\nu}_s)(1 + \Gamma)W_T, \tag{B1}$$

where W_T is half of the tracer permeability of a single boundary layer.

The experimental transport properties of the membrane, measured in the presence of boundary layers, are based on the bulk solution concentration difference Δc_s. As indicated earlier, these coefficients are primed. Properties based on the true transmembrane concentration difference Δc_m are unprimed. The primed and unprimed phenomenological permeabilities are defined accordingly by Def. 2

$$\omega_P' RT = -\left(\frac{J_s}{\Delta c_s}\right)_{J_v=0} = -\left(\frac{J_s}{\Delta c_m}\right)_{J_v=0}\left(\frac{\Delta c_m}{\Delta c_s}\right)_{J_v=0} = \omega_P RT\left(\frac{\Delta c_m}{\Delta c_s}\right)_{J_v=0}. \tag{B2}$$

The ratio $(\Delta c_m/\Delta c_s)_{J_v=0}$ is found from the flux equations for transport across the membrane alone (Eq. I1 *a* and *b* with Δc_m replacing Δc_s) and the equation for solute flux across the boundary layers (7); the last of these is

$$J_s = J_v \bar{c}_s - W_P RT(\Delta c_s - \Delta c_m).$$

Equating the solute flux across the boundary layers and that across the membrane, and solving for Δc_m:

$$\Delta c_m = \frac{W_P RT \Delta c_s - J_v \sigma_s \bar{c}_s}{RT(W_P + \omega_P)}. \tag{B3}$$

When $J_v = 0$,

$$\left(\frac{\Delta c_m}{\Delta c_s}\right)_{J_v=0} = \frac{W_p}{W_P + \omega_P}. \tag{B4}$$

Combining Eqs. B2 and B4 and rearranging,

$$\omega_P = \frac{\omega_P' W_P}{W_P - \omega_P'}. \tag{B5}$$

Similarly, from the definitions of σ_v and σ_v',

$$\sigma_v = \frac{\sigma_v'(W_P + \omega_P)}{W_P}. \tag{B6}$$

It was shown in reference 7 that the ratio σ_s'/σ_v' equals σ_s/σ_v; therefore,

$$\sigma_s = \frac{\sigma_s'(W_P + \omega_P)}{W_P}. \tag{B7}$$

The experimental hydraulic conductivity is defined by Def. 4. Using Eqs. I1 *a*, B3, B6, and B7,

$$L_p = \frac{L_p'}{1 - \dfrac{\sigma_v' \sigma_s'(W_P + \omega_P) L_p' \bar{c}_s}{W_P^2}}. \tag{B8}$$

The tracer permeabilities of the membrane and the boundary layers can be regarded as conductances in series; thus,

$$\frac{1}{\omega'_T} = \frac{1}{W_T} + \frac{1}{\omega_T}; \omega_T = \frac{\omega'_T W_T}{W_T - \omega'_T}. \tag{B9}$$

Substituting Eqs. B1, B5, B6, B8, B9, and $\sigma'_s = \sigma'_v(1 - \bar{\nu}_s)/(1 + \Gamma)$ into Eq. 8 *a*,

$$\omega'_P = \frac{(1 - \bar{\nu}_s)(1 + \Gamma + \sigma'_v\bar{\nu}_s)^2}{(1 + \Gamma)\left(1 - \dfrac{\omega'_T\bar{\nu}_s^2}{L'_p\bar{c}_s}\right)}\omega'_T. \tag{B10}$$

This relationship among the experimental transport coefficients, measured with boundary layers present, is the same as Eq. 8 *a* for a homoporous membrane without boundary layers.

APPENDIX C

Phenomenological Solute Permeability of a Three-Path Membrane

The objective here is to select values of L_{pi}, σ_{si}, and ω_{Ti} such that (*a*) the experimental L_p, σ_s and ω_T of the composite have prescribed values and (*b*) ω_P (as given by Eq. 14) is large. This will be done first for the boundary-layer-free case.

As observed earlier, the effect of heteroporosity on ω_P that is found even in ideal dilute solutions derives from the bracketed term in Eq. 14. This term is maximized by setting the solute flow reflection coefficient of the first path, σ_{s1}, equal to unity, and $L_{p1} = L'_p\sigma'_s$, exactly as for the two-path membrane.

Since $L_{pi}\sigma_{s1} = L'_p\sigma'_s$, it follows from Eq. 11 *d* that $\Sigma_{i>1}L_{pi}\sigma_{si} = 0$, or, since neither L_{pi} nor σ_{si} are negative, $L_{pi}\sigma_{si} = 0$, $i > 1$. Since ω_{Ti}/L_{pi} is bounded (Appendix A), $\omega_{Ti} = 0$ for all paths whose $L_{pi} = 0$, and such "paths," which prohibit transport entirely, do not contribute to either sum in Eq. 14. For those additional paths that may contribute, $\sigma_{si} = 0$; thus, $L_{pi}\sigma_{si}^2 = 0$ for these paths, and $\omega_{Pi} = \omega_{Ti}(1 + \Gamma)(1 - \bar{\nu}_s)/[1 - \omega_{Ti}\bar{\nu}_s^2/(L_{pi}\bar{c}_s)]$. For any ω_{T2}, ω_{P2} is maximized if L_{p2} is such that $\omega_{T2}\bar{\nu}_s^2/(L_{p2}\bar{c}_s)$ equals its upper limit, $\bar{\nu}_s$; it can be shown *a posteriori*, using the experimental data of Meyer et al. (6), that if $\omega_{T2} = \omega'_T$, $L_{p2} = \omega_{T2}\bar{\nu}_s/\bar{c}_s$, and $L_{p1} = L'_p\sigma'_s$, then $L_{p1} + L_{p2} < L'_p$, so Eq. 11 *a* is not violated. Assigning these values to ω_{T2} and L_{p2}, $\omega_{P2} = \omega'_T(1 + \Gamma)$. The second path is nonselective and is the solute pathway.

To satisfy the conservation equations, a third path must exist for which $L_{p3} = L'_p - L_{p1} - L_{p2}$, $\sigma_{s3} = 0$, and $\omega_{T3} = 0$. This is strictly forbidden by Eqs. 4 and I7, but it is possible to show that a path can exist whose hydraulic conductivity is positive, whose reflection coefficient is zero, and whose tracer permeability is arbitrarily small. The contribution of such a path to the sums in Eq. 14 is likewise arbitrarily small.

From Eq. 14, the phenomenological permeability of the model heteroporous membrane described above is:

$$\begin{aligned}\omega_P^{(3)} &= \left(\frac{1 + \Gamma}{1 - \nu_s}\right)L'_p\bar{c}_s\sigma'_s(1 - \sigma'_s) + \omega'_T(1 + \Gamma)\\ &= L'_p\bar{c}_s\sigma'_v(1 - \sigma'_s) + \omega'_T(1 + \Gamma).\end{aligned} \tag{16}$$

This expression differs from that for the maximum phenomenological permeability of a heteroporous membrane in ideal dilute solutions (3) in two ways: a distinction is made between σ'_v and σ'_s, and an additional $\Gamma\omega'_T$ term appears on the right-hand side.

Since the model membrane considered here appears to maximize ω_P, the effect of boundary layer thickness on the phenomenological solute permeability of such an array merits examination. We use unprimed variables to denote the properties of the composite which would be measured in the absence of

a boundary layer. These properties are related to the properties of each path through Eq. 11 *a–d* and to the (primed) experimental properties through Eqs. B5–B9.

Consider again the three-path heteroporous membrane whose individual paths are such that its composite (boundary-layer-free) properties are related by Eq. 16: $\omega_P^{(3)} = L_p\bar{c}_s\sigma_v(1 - \sigma_s) + \omega_T(1 + \Gamma)$. Using Eqs. B1 and B6–B9, the right-hand side of this expression can be written in terms of the experimental properties which the composite must exhibit:

$$\omega_P^{(3)} = \frac{L'_p\bar{c}_s\sigma'_v(W_P + \omega_P^{(3)})[W_P - \sigma'_s(W_P + \omega_P^{(3)})]}{W_P^2 - \sigma'_v\sigma'_s(W_P + \omega_P^{(3)})L'_p\bar{c}_s} + \frac{\omega'_T W_P(1 + \Gamma)}{W_p - (1 - \bar{\nu}_s)(1 + \Gamma)\omega'_T}. \quad \text{(C1)}$$

From Eq. B5, the experimental phenomenological permeability of the composite is related to the boundary-layer-free value by

$$\omega'^{(3)}_P = \frac{\omega_P^{(3)} W_P}{W_P + \omega_P^{(3)}}; \quad \text{(C2)}$$

solving Eq. C1 for $\omega_P^{(3)}$ and substituting into Eq. C2,

$$\omega'^{(3)}_P = L'_p\bar{c}_s\sigma'_v(1 - \sigma'_s) + \omega'_T(1 + \Gamma)\left[\frac{W_P - L'_p\bar{c}_s\sigma'_v}{W_p + \bar{\nu}_s(1 + \Gamma)\omega'_T}\right].$$

The bracketed term above is always less than unity; as the boundary layer becomes thinner ($W_p \to \infty$), the experimentally measured phenomenological solute permeability of the model three path membrane, $\omega'^{(3)}_P$, approaches from below that predicted from the boundary-layer-free analysis.

Received for publication 23 July 1980 and in revised form 27 January 1981.

REFERENCES

1. Katchalsky, A., and O. Kedem. 1962. Thermodynamics of flow processes in biological systems. *Biophys. J.* 2:53–78.
2. Patlak, C. S., and S. I. Rapoport. 1971. Theoretical analysis of net tracer flux due to volume circulation in a membrane with pores of different sizes. *J. Gen. Physiol.* 57:113–124.
3. Friedman, M. H. 1976. The effect of membrane heterogeneity on the predictability of fluxes, with application to the cornea. *J. Theor. Biol.* 61:307–328.
4. Li, J. H., and A. Essig. 1976. Influence of membrane heterogeneity on kinetics of nonelectrolyte tracer flows. *J. Membr. Biol.* 29:255–264.
5. Kedem, O., and A. Katchalsky. 1963. Permeability of composite membranes. 2. Parallel elements. *Trans. Faraday Soc.* 59:1931–1940.
6. Meyer, R. A., E. C. Hills, and M. H. Friedman. 1981. Tracer permeabilities underestimate transmembrane solute flux under a concentration gradient. *J. Membr. Sci.* In Press.
7. Friedman, M. H., and R. A. Meyer. 1981. Transport across homoporous and heteroporous membranes in nonideal, nondilute solutions. I. Inequality of reflection coefficients for volume flow and solute flow. *Biophys. J.* 34:535–544.
8. Kedem, O., and A. Katchalsky. 1961. A physical interpretation of the phenomenological coefficients of membrane permeability. *J. Gen. Physiol.* 45:143–179.
9. Meyer, R. A., and M. H. Friedman. 1977. Interferometric technique for the simultaneous measurement of passive membrane transport coefficients. *Rev. Sci. Instrum.* 48:1317–1321.
10. Lightfoot, E. N. 1974. Transport phenomena and living systems. John Wiley & Sons, Inc., New York.
11. Katchalsky, A., and P. F. Curran. 1965. Nonequilibrium thermodynamics in biophysics. Harvard University Press, Cambridge, Massachusetts.